

**ELUCIDATING THE EFFECTS OF mTOR
INHIBITORS FROM MALAYSIAN NATURAL
PRODUCTS ON TUBEROUS SCLEROSIS
COMPLEX CELL LINE**

NINIE NADIA BINTI ZULKIPLI

UNIVERSITI SAINS MALAYSIA

2022

**ELUCIDATING THE EFFECTS OF mTOR
INHIBITORS FROM MALAYSIAN NATURAL
PRODUCTS ON TUBEROUS SCLEROSIS
COMPLEX CELL LINE**

by

NINIE NADIA BINTI ZULKIPLI

**Thesis submitted in fulfilment of the requirements
for the Degree of
Doctor of Philosophy**

February 2022

ACKNOWLEDGEMENT

In the name of Allah, the Most Gracious and the Most Merciful. Alhamdulillah, thank you Allah for all the blessing You had given me. First and foremost, I would like to show my deepest appreciation to my supervisor, Assoc. Professor Dr. Rahimah Zakaria for her valuable and endless support and guidance throughout of this study. Her continuous motivation and enthusiastic supervision regardless of the time towards the completion of this thesis inspired me to do my best. Her wide knowledge and great assistance are precious for me throughout of this journey. I also would like to convey my deepest gratitude as well to my co-supervisors, Assoc. Professor Dr. Teguh Haryo Sasongko, Professor Dr. Habibah A Wahab and Dr. Idris Long for their great assistance, kind supervision and motivation regardless of the distance and time. I would like to acknowledge Research University Grant (RUI) for funding this research through Grant Scheme (1001/PPSP/812137) and Ministry of Education (MOE) for awarding me the MyBrainSc scholarship from 2017-2020. Not forgotten, thank you very much to Human Genome Centre (HGC), Central Research Laboratory and Craniofacial Laboratory for providing all needed facilities for my study. Many thanks to HGC members especially Director of HGC, Assoc. Professor Dr. Sarina Sulong for improving my skills throughout of this study. Not forgotten to HGC students; Shafawati, Ikah, Dr. Wan Khairunnisa, Maziras, Fazreen, Sabrina and Syidah for their valuable discussion and continuous support throughout of this study period. Last but not least, I extend my deepest gratitude goes to my beloved parents; Mr. Zulkipli Muhammad and Mrs. Zah Zain and also to my sisters and brother for their prayers, assistance, endless love and encouragement.

Ninie Nadia Zulkipli, June 2021

TABLE OF CONTENTS

ACKNOWLEDGEMENT	ii
TABLE OF CONTENTS	iii
LIST OF TABLES	vii
LIST OF FIGURES	x
LIST OF SYMBOLS AND ABBREVIATIONS	xiv
LIST OF APPENDICES	xxv
ABSTRAK	xxvi
ABSTRACT	xxviii
CHAPTER 1 INTRODUCTION	1
1.1 Research background	1
1.2 Rationale of the study	3
1.3 Objectives of the study	4
1.3.1 General objective	4
1.3.2 Specific objectives	4
CHAPTER 2 LITERATURE REVIEW	5
2.1 Tuberous Sclerosis Complex (TSC)	5
2.2 TSC genes, their protein products and TSC protein complex	7
2.3 mTOR complexes and their function	11
2.4 Clinical features and classification of TSC	16
2.5 The mTOR signalling pathway of TSC	18
2.6 Therapeutic options for TSC	21
2.6.1 First-generation mTOR inhibitors	21
2.6.2 Second-generation mTOR inhibitors	34
2.6.3 Dual PI3K/mTOR inhibitors	38
2.6.4 Third-generation mTOR inhibitors	44
2.7 NADI database	47
2.8 Drug discovery and development	48
2.8.1 Traditional drug discovery and development	48
2.8.2 Modern drug discovery and development based on in silico approaches	49
2.8.2 (a) Molecular docking	53
2.8.2 (b) Virtual screening	56
2.9 Cytotoxicity evaluation	57

2.10	Reverse transcription quantitative real-time polymerase chain reaction (RT-qPCR)	59
CHAPTER 3	MATERIALS AND METHODS	64
3.1	Study design	64
3.2	Materials	66
3.2.1	Cell line	66
3.2.2	Substances	66
3.2.3	Chemicals and reagents	67
3.2.4	Kits and assays	68
3.2.5	Consumables	69
3.2.6	Laboratory equipment	70
3.2.7	Computer programs, software and databases	71
3.3	Preparation of reagents and buffers	72
3.3.1	Preparation of PBS (1x)	72
3.3.2	Preparation of complete medium	72
3.3.3	Preparation of 1x TAE buffer	72
3.3.4	Preparation of 70% ethanol	73
3.3.5	Preparation of 100X SYBR Green I	73
3.3.6	Preparation of RNA ladder	73
3.3.7	Preparation of 1% agarose gel	74
3.4	Stage 1: In silico approaches	74
3.4.1	Accession of the target protein	76
3.4.2	Ligand selection	76
3.4.3	Analysis of target active binding sites	77
3.4.4	Control docking procedure	77
3.4.5	Virtual screening	78
3.4.6	Molecular docking analysis	78
3.5	Stage 2: Determination of IC ₅₀ of selected substances	79
3.5.1	Thawing of frozen UMB1949 cell line	79
3.5.2	Maintenance of UMB1949 cell line	80
3.5.3	Subculture of UMB1949 cell line	80
3.5.4	Cell count with hemocytometer	81
3.5.5	Cryopreservation of cell cultures	84
3.5.6	Serial dilution of drug substances	84
	3.5.6 (a) Everolimus serial dilution	84
	3.5.6 (b) Asiaticoside serial dilution	85

3.5.6 (c) Asiatic acid serial dilution	85
3.5.7 Calculation of cell viability	85
3.5.8 Determination of half-maximal inhibitory concentration (IC ₅₀) values	86
3.6 Stage 3: mTOR pathway profiling by reverse transcription quantitative real-time polymerase chain reaction (RT-qPCR)	87
3.6.1 Preparation of cells for total RNA extraction	87
3.6.2 Protocols for total RNA extraction	88
3.6.3 Total RNA qualification and quantification	89
3.6.4 Protocol for agarose gel electrophoresis	90
3.6.5 Protocol for cDNA synthesis	90
3.6.6 Gene expression using reverse transcription quantitative real-time polymerase chain reaction (RT-qPCR)	92
3.6.6 (a) Profiling of reference genes (RGs) and genes of interest (GOIs)	93
3.6.6 (b) Serial dilution of cDNA	95
3.7 Functional and pathway enrichment analysis of DEGs	97
3.8 Validation of the gene expression for selected genes found to be highly modulated along the mTOR pathway	97
3.8.1 Relative quantification analysis	100
3.9 Statistical analysis	101
CHAPTER 4 RESULT	102
4.1 Molecular docking	102
4.2 The half-maximal inhibitory concentration (IC ₅₀) of substances	114
4.2.1 Everolimus	114
4.2.2 Asiaticoside	115
4.2.3 Asiatic acid	116
4.3 mTOR profiling by RT-qPCR	118
4.3.1 Total RNA qualification and quantification	118
4.3.2 Reverse transcription quantitative real-time polymerase chain reaction (RT-qPCR)	119
4.3.3 mTOR profiling to determine the reference genes (RGs)	120
4.3.4 mTOR profiling to determine the genes of interest (GOIs)	124
4.3.4 (a) Gene expression profiling in response to everolimus	124
4.3.4 (b) Gene expression profiling in response to asiaticoside	128
4.3.4 (c) Gene expression profiling in response to asiatic acid	131

4.4	Enriched GO terms and pathways	133
4.5	Selection of genes of interest (GOIs)	149
4.6	Primer specificity and efficiency by reverse transcription quantitative real-time polymerase chain reaction (RT-qPCR)	153
4.6.1	PCR efficiency	153
4.6.2	Amplification of reference genes (RGs) and genes of interest (GOIs)	153
CHAPTER 5 DISCUSSION		159
5.1	In silico analyses revealed potential mTOR inhibitors originating from Malaysian natural substances	159
5.2	Cytotoxicity study of everolimus and potential mTOR inhibitors from natural products on the UMB1949 cell line	165
5.3	Identification of ideal reference genes (RGs) for normalisation of gene expression by using reverse transcription quantitative real-time polymerase chain reaction (RT-qPCR)	167
5.4	Expression analysis of selected genes of interest (GOIs) in mTOR pathway of UMB1949 cell line	169
5.5	Bioinformatics analysis of DEGs	175
5.6	GO analysis of the identified significant DEGs	178
CHAPTER 6 CONCLUSION, LIMITATIONS AND RECOMMENDATIONS		185
6.1	Conclusion	185
6.3	Limitations of the study and recommendations for future research	188
REFERENCES		190
APPENDICES		
LIST OF PUBLICATIONS		
LIST OF PRESENTATIONS		

LIST OF TABLES

		Page
Table 2.1	Revised and updated clinical diagnostic criteria of TSC	17
Table 2.2	The pharmacology of the first-generation mTOR inhibitors	25
Table 3.1	Details of cell line	66
Table 3.2	The list of substances	66
Table 3.3	The list of chemicals and reagents	67
Table 3.4	The list of kits and assay	68
Table 3.5	The list of consumables	69
Table 3.6	The list of laboratory equipment	70
Table 3.7	The list of computer programs, software and databases	71
Table 3.8	Genomic DNA elimination mix	91
Table 3.9	Reverse-transcription mix	91
Table 3.10	PCR components mix	93
Table 3.11	Cycling condition for Stratagene	95
Table 3.12	PCR components mix for determination of PCR amplification efficiency of each gene	96
Table 3.13	Cycling condition for determination of PCR amplification efficiency of each gene	96
Table 3.14	The details of primers for RGs and GOIs used RT-qPCR analysis	98
Table 3.15	PCR components mix for one reaction	99
Table 3.16	Cycling condition for validation of gene expression for selected genes in mTOR pathway	99

Table 3.17	The formula for comparative ($\Delta\Delta C_t$) method	101
Table 4.1	The top hits from the NADI virtual screen, grouped according to the associated plants source	103
Table 4.2	The docking scores and interaction analysis of each ligand in complex with FKBP5 and FRB domains of human proteins	112
Table 4.3	The formula for calculated docking score of everolimus by AutoDock 4.2.6	112
Table 4.4	The formula for calculated docking score of asiaticoside by AutoDock 4.2.6	113
Table 4.5	The formula for calculated docking score of asiatic acid by AutoDock 4.2.6	113
Table 4.6	The C_t values resulted from mTOR profiling of each proposed RGs for specific groups	122
Table 4.7	The average value of geometric mean for each group based on C_t values of three RGs	123
Table 4.8	The relative mRNA expression levels of genes after 24 hours of everolimus exposure	127
Table 4.9	The relative mRNA expression level of genes after 24 hours of asiaticoside exposure	130
Table 4.10	The relative mRNA expression level of genes after 24 hours of asiatic acid exposure	133
Table 4.11	The details of top five GO analysis and pathway enrichment for DEGs treated with everolimus	136
Table 4.12	The details of top five GO analysis and pathway enrichment for DEGs treated with asiaticoside	142
Table 4.13	The details of GO analysis and pathway enrichment of DEGs treated with asiatic acid	148
Table 4.14	The C_t values of three RGs obtained from validation experiments across the treatment and control groups	155
Table 4.15	The validation of GOIs for the everolimus group	156

Table 4.16	The validation of GOIs for the asiaticoside group	157
Table 4.17	The validation of GOIs for the asiatic acid group	158
Table 5.1	Physicochemical properties of the substances	162
Table 5.2	Summary of functional analyses and KEGG pathway of DEGs treated everolimus, asiaticoside and asiatic acid	179

LIST OF FIGURES

		Page
Figure 2.1	The detailed structures of hamartin and tuberlin	8
Figure 2.2	The subunits of TSC protein complex, mTORC1 subunits and its downstream functions	11
Figure 2.3	Schematic representation of mTOR domain	12
Figure 2.4	mTOR complexes: mTORC1 and mTORC2 mTOR forms two distinct structurally and functionally complexes: mTORC1 and mTORC2	15
Figure 2.5	The inputs and downstream functions in the mTOR pathway that responsible for TSC	18
Figure 2.6	The chemical structures of first-generation mTOR inhibitors	32
Figure 2.7	Illustration of mechanism action for rapamycin and its rapalogs	33
Figure 2.8	The mechanism of action of rapamycin and its rapalogs that responsible for inhibiting the downstream of mTOR	34
Figure 2.9	The chemical structure of second-generation mTOR inhibitors	37
Figure 2.10	The general mechanism of action of mTOR inhibitors	38
Figure 2.11	The chemical structure of dual PI3K/mTOR inhibitor	42
Figure 2.12	The structure of the third-generation mTOR inhibitor	45
Figure 2.13	The diagram illustrated the steps involved in traditional drug discovery and development	48
Figure 2.14	The diagram illustrated the full phases for manufacturing a new drug in modern drug discovery	51

Figure 2.15	Illustration reaction for the detection of dehydrogenase activity in WST-8 assay	59
Figure 3.1	The flowchart of the study	65
Figure 3.2	The flowchart of in silico approach applied in this present study	75
Figure 3.3	Hemocytometer diagram showing one of the sets of 16 squares that need to be used for counting	83
Figure 3.4	The continuous and dotted lines indicated counted and uncounted area, respectively for viable cells	83
Figure 3.5	The RT ² profiler PCR array of mTOR pathway consists of 84 genes and RGs that involve in the mTOR pathway, genomic DNA control, reverse transcription controls and positive PCR controls	94
Figure 4.1	Binding modes comparison between crystallographic structure (rapamycin; grey colour) and the lowest energy dock modes of everolimus (purple colour); asiaticoside (orange colour); asiatic acid (yellow colour), respectively	109
Figure 4.2	The interactions formed between each ligand (everolimus - purple colour; asiaticoside - orange colour; asiatic acid - yellow colour) and specific amino acid residues of FKBP5 and FRB-domain mTOR of human proteins	111
Figure 4.3 (a)	Chemical structure of everolimus	114
Figure 4.3 (b)	Everolimus showed anti-proliferative effects on the UMB1949 cell line	114
Figure 4.4 (a)	Chemical structure of asiaticoside	115
Figure 4.4 (b)	Asiaticoside manifests anti-proliferative effects on the UMB1949 cell line	115
Figure 4.5 (a)	Chemical structure of asiatic acid	116
Figure 4.5 (b)	Asiatic acid exhibits anti-proliferative effects on the UMB1949 cell line	116

Figure 4.6	The effect of each treatment on the UMB1949 cell line after 24 hours	117
Figure 4.7	Represented of total RNA extracted from control group and treatment groups	119
Figure 4.8	The heat map diagram shows the relative mRNA expression levels of DEGs post-everolimus treatment according to the RT ² profiler PCR array format of mTOR pathway	125
Figure 4.9	Statistically significant relative mRNA expression levels of genes in the mTOR pathway after 24 hours of everolimus exposure	126
Figure 4.10	The heat map diagram illustrates the relative mRNA expression levels of DEGs post-asiaticoside treatment according to the RT2 profiler PCR array format of mTOR pathway	128
Figure 4.11	Statistically significant relative mRNA expression levels of genes in the mTOR pathway after 24 hours of asiaticoside exposure	129
Figure 4.12	The heat map diagram illustrates the relative mRNA expression levels of DEGs post-asiatic acid treatment according to the RT2 profiler PCR array format of mTOR pathway	132
Figure 4.13	Statistically significant gene expression in the mTOR pathway after 24 hours of asiatic acid exposure	132
Figure 4.14	Bar graphs of top-five and significantly (p-value < 0.05 and count > 2) enriched GO terms of ontologies and KEGG pathways for DEGs treated with everolimus	135
Figure 4.15	Top five GO terms of ontologies (biological process, molecular function and cellular component) and KEGG pathways of DEGs treated with asiaticoside	141

Figure 4.16	Functional analyses and KEGG pathway of DEGs treated with asiatic acid	147
Figure 4.17	Venn diagram of upregulated and downregulated DEGs according to each treatment group where purple, orange and yellow represented everolimus, asiaticoside and asiatic acid, respectively	150
Figure 4.18	The upregulated genes expressed in the similar treatment groups	151
Figure 4.19	The downregulated genes expressed in similar and different treatment groups	152
Figure 4.20	In everolimus group, <i>CAB39</i> , <i>PRKCE</i> , <i>RRAGC</i> and <i>RPS6KA5</i> showed upregulation of relative mRNA expression levels while <i>DEPTOR</i> and <i>IGFBP3</i> displayed downregulation of relative mRNA expression levels	156
Figure 4.21	In asiaticoside group, <i>CAB39</i> , <i>PRKCE</i> , <i>RRAGC</i> and <i>RPS6KA5</i> showed upregulation of relative mRNA expression levels while <i>DEPTOR</i> and <i>VEGFC</i> showed downregulation of relative mRNA expression levels	157
Figure 4.22	In asiatic acid group, <i>CAB39</i> , <i>PRKCE</i> , <i>RRAGC</i> and <i>RPS6KA5</i> showed upregulation of relative mRNA expression levels while <i>DEPTOR</i> and <i>IGFBP3</i> showed downregulation of relative mRNA expression levels	158
Figure 5.1	Overview of the mTOR signalling pathway	183

LIST OF SYMBOLS AND ABBREVIATIONS

-	Minus
%	Percentage
°C	Degree celcius
+	Plus
<	Less than
>	Greater than
±	Plus minus
µg	Microgram
µL	Microlitre
µM	Micromolar
α	Alpha
<i>β</i> -met	<i>β</i> -mercaptoethanol
Δ	Delta
δ	Delta
ε	Epsilon
ζ	Zeta
η	Eta
Å	Angstrom
4EBP	4E binding protein
A260/A230	Absorbance at 260 nm and 230 nm
A260/A280	Absorbance at 260 nm and 280 nm
AA	Adjuvant arthritis
ADME	Absorption, distribution, metabolism and elimination

AML	Acute myeloid leukemia
AMP	Adenosine monophosphate
AMPK	AMP-activated protein kinase
ATCC	American Type Culture Collection
Atg101	Autophagy-related protein 101
Atg13	Autophagy-related protein 13
ATP	Adenosine triphosphate
BP	Biological process
Bp	Base pair
Buffer RLT	Lysis buffer
Buffer RPE	Washing buffer
Buffer RW1	Washing buffer
C40	Carbon 40
CAB39	Calcium binding protein 39
CAB39L	Calcium binding protein 39-like
CADD	Computer-aided drug design
CC	Cellular components
CCK-8	Cell counting kit-8
cDNA	Complementary DNA
CHUK	Conserved helix-loop-helix ubiquitous kinase
C _t	Cycle threshold
DAVID	Database for Annotation, Visualization and Integrated Discovery
DDIT4	DNA-damage-inducible transcript 4
DDIT4L	DNA-damage-inducible transcript 4-like

DEGs	Differentially expressed genes
DEPTOR	DEP domain containing MTOR-interacting protein
DMEM	Dulbecco's Modified Eagle Medium
DMSO	Dimethyl sulfoxide
DNA	Deoxyribonucleic acid
DNase	Deoxyribonuclease
dsDNA	Double-stranded DNA
EAE	Experimental allergic encephalomyelitis
EASE	Expression Analysis Systematic Explorer, the modified Fisher Exact p-value
EBV	Epstein-Barr virus
ECM	Extracellular matrix
EGF	Epidermal growth factor
EIF4B	Eukaryotic translation initiation factor 4B
eIF4E	Eukaryotic initiation factor 4E
EIF4EBP2	Eukaryotic translation initiation factor 4E binding protein 2
EMA	European Medicines Agency
EMT	Epithelial to mesenchymal transition
ERK	Extracellular-signal-regulated kinase
ERM	Ezrin-radixin-moesin
ESCC	Esophageal squamous cell carcinoma
ETS	E26 transformation–specific
ETV7	ETS variant transcription factor 7
FAT	FRAP, ATM and TRRAP
FATC	FAT C-terminus

FBS	Fetal Bovine Serum
FIP200	Focal adhesion kinase family interacting protein of 200 kDa
FKBP12	12-kDa FK506-binding protein
FKBP5	FK506-binding protein 5
FoxO	Forkhead box O
FRB-domain	FKBP12-rapamycin-binding domain
g	Gram
g/mol	Gram per molecule
GAP	GTPase-activating protein
GAPDH	Glyceraldehyde-3-phosphate dehydrogenase
G-CSF	Granulocyte colony-stimulating factor
GDC	Genomic DNA control
GDP	Guanosine diphosphate
GO	Gene Ontology
GOIS	Genes of interest
Grb10	Growth factor receptor-bound protein 10
GSK3B	Glycogen synthase kinase 3 beta
GTP	Guanosine triphosphate
H5N1/H1N1	Highly Pathogenic Asian Avian Influenza A/ Hemagglutinin Type 1 and Neuraminidase Type
HEAT	Huntington, Elongation factor 3A, A subunit of PP2A, and TOR1
HER2	Human epidermal growth factor receptor 2
HIF	Hypoxia-inducible factor
HIV	Human immunodeficiency virus
HNSCC	Head and neck squamous cell carcinoma

HPRT1	Hypoxanthine phosphoribosyltransferase 1
HR	Hormone-receptor
HTLV-1	Human T- cell leukemia virus, type 1
HTS	High-throughput screening
IC ₅₀	Half-maximal inhibitory concentration
IgE	Immunoglobulin E
IGF	Insulin-like growth factor
IGF-1R	Insulin-like growth factor-1 receptor
IGFBP3	Insulin-like growth factor binding protein 3
IKBKB	Vascular endothelial growth factor A
IL-12	Interlukin-12
IL-2	Interlukin-2
Ile	Isoleucine
INSR	Insulin receptor
IR	Insulin receptor
IRS	Insulin receptor substrate
kb	Kilo base
kcal/mol	Kilocalorie per mole
kDa	Kilo Dalton
KEGG	Kyoto Encyclopedia of Genes and Genomes
LAM	Lymphangioleiomyomatosis
LBDD	Ligand-based drug design
LBVS	Ligand-based virtual screening
Leu	Leucine

LGA	Lamarckian Genetic Algorithm
LKB1	Liver kinase B1
MAP4K3	Mitogen-activated protein kinase 3
MAPK	Mitogen-activated protein kinase
MAPK1	Mitogen-activated protein kinase 1
MCL	Mantle cell lymphoma
mCRPC	Metastatic castration-resistant prostate cancer
MD	Molecular dynamics
MF	Molecular function
mg	Milligram
mL	Millilitre
mLST8	Mammalian lethal with Sec13 protein 8
MO25	Mouse protein-25
MPM	Malignant pleural mesothelioma
mRNA	Messenger ribonucleic acid
mSIN-1	Mammalian stress-activated protein kinase interacting protein
MSK1	Mitogen- and stress-activated protein kinase 1
MSK2	Mitogen- and stress-activated protein kinase 2
mTOR	Mammalian target of rapamycin
mTORC1	Mammalian target of rapamycin complex 1
mTORC2	Mammalian target of rapamycin complex 2
mTORC3	Mammalian target of rapamycin complex 3
MTT	3-(4,5-dimethylthiazol-2-yl)-2,5-diphenyl tetrazolium bromide
NADH	Nicotinamide adenine dinucleotide

NADI	Natural Product Discovery
NADPH	Nicotinamide adenine dinucleotide phosphate
NF-kB	Nuclear factor-kappa B
ng	Nanogram
ng/μL	Nanogram per microlitre
nm	Nanometer
NMR	Nuclear magnetic resonance
NPRA	National Pharmaceutical Regulatory Agency
NSCLC	Non-small-cell lung cancer cell lines
NTC	No template control
OD	Optical density
p.	Protein
PBS	Phosphate Buffer Saline
PCR	Polymerase chain reaction
PDB	Protein data bank
PDBQT	Protein data bank (PDB) format file plus partial charges (q) and torsion angles (t)
PDK2	Phosphoinositide-dependent kinase 2
PDPK1 (PDK1)	3-phosphoinositide dependent protein kinase-1
PFS	Progression-free survival
Phe	Phenylalanine
PI3K	Phosphoinositide 3kinase
PIK3CA	Phosphoinositide-3-kinase, catalytic, alpha polypeptide
PIK3CB	Phosphoinositide-3-kinase, catalytic, beta polypeptide
PIK3CG	Phosphoinositide-3-kinase, catalytic, gamma polypeptide

PIKKs	Phosphatidylinositol 3-kinase-related kinases
PIP2	Phosphatidylinositol 4,5-bisphosphate
PIP3	Phosphatidylinositol (3,4,5)-trisphosphate
PKC	Protein kinase C
PMS	Phenazinium methylsulfate
PNETs	Pancreatic neuroendocrine tumours
PNT	Pointed
PPC	Positive PCR controls
PRAS40	Proline-rich AKT substrate of 40kDa
PRKAA2	Protein kinase, AMP-activated, alpha 2 catalytic subunit
PRKAB1	Protein kinase, AMP-activated, beta 1 non-catalytic subunit
PRKAB2	Protein kinase, AMP-activated, beta 2 non-catalytic subunit
PRKAG1	Protein kinase, AMP-activated, gamma 1 non-catalytic subunit
PRKCE	Protein kinase C, epsilon
PROTOR-1	Protein observed with RICTOR-1
QC	Quality control
qPCR	Quantitative real-time polymerase chain reaction
QSAR	Quantitative structure-activity relationship
R ²	Correlation coefficient
Raptor	Regulatory-associated protein of mTOR
RCC	Renal cell carcinoma
REDD1/2	Regulated in Development and DNA Damage Responses - 1/2
RGs	Reference genes
Rheb	Ras homolog enriched in brain

Rictor	Rapamycin-insensitive companion of mTOR
RMSD	Root-mean-square deviation
RNA	Ribonucleic acid
RNase	Ribonuclease
rpm	Revolution per minute
RPS6KA1	Ribosomal protein S6 kinase, 90kDa, polypeptide 1
RPS6KA5	Ribosomal protein S6 kinase, 90kDa, polypeptide 5
RRAGB	Ras-related GTP binding B
RRAGC	Ras-related GTP binding C
RRAGD	Ras-related GTP binding D
rRNA	Ribosomal ribonucleic acid
RSK	Ribosomal protein-S6 kinase
RTC	Reverse transcription controls
RTKs	Receptor tyrosine kinases
RT-PCR	Qualitative reverse transcription polymerase chain reaction
RT-qPCR	Reverse transcription quantitative real-time polymerase chain reaction
S473	Serine 473
S475	Serine 475
S6K1	S6 kinase 1
SBDD	Structure-based drug design
SBVS	Structure-based virtual screening
SD	Standard deviation
SEGA	Subependymal giant cell astrocytoma
SGK1	Serum and glucocorticoid regulated kinase 1

ssRNA	Single-stranded RNA
STRAD α	STE20 Related Adaptor Alpha
STS	Soft tissue sarcomas
SUCCEED	Sarcoma Multicenter Clinical Evaluation of the Efficacy of Ridaforolimus
SV40	Simian virus 40
T1135	Threonine 1135
T25	25 cm ² cell culture flask
T308	Threonine 308
T389	Threonine 389
TAE	Tris-acetate-EDTA
TBC1D7	Tre2-Bub2-Cdc16 (TBC) 1 domain family, member 7
TCL	T-cell lymphoma
Trp	Tryptophan
TSC	Tuberous sclerosis complex
TSC1	Tuberous sclerosis complex 1
TSC2	Tuberous sclerosis complex 2
Tyr	Tyrosine
ULK1/2	Unc-51-like kinase 1/2
USFDA	United States Food and Drug Administration
USM	Universiti Sains Malaysia
UV	Ultraviolet
V	Volts
Val	Valine
VEGF	Vascular endothelial growth factor

VEGFA	Vascular endothelial growth factor A
VEGFC	Vascular endothelial growth factor C
VEGFR-2	Vascular Endothelial Growth Factor Receptor-2
VEGFR-3	Vascular Endothelial Growth Factor Receptor-3
vHTS	Virtual high throughput screening
VLA-4	Very late antigen-4
VPS34	Phosphatidylinositol 3-kinase VPS34
WST-1	Water-Soluble Tetrazolium 1
WST-8	Water-Soluble Tetrazolium 8

LIST OF APPENDICES

APPENDIX A	Certificate of analysis UMB1949 cell line
APPENDIX B	Datasheet of everolimus
APPENDIX C	Datasheet of asiaticoside
APPENDIX D	Datasheet of asiatic acid
APPENDIX E	Terms in reverse transcription quantitative real-time polymerase chain reaction (RT-qPCR)
APPENDIX F	Standard curve of PCR primer efficiency for selected genes
APPENDIX G	Amplification curves and melting curves for selected genes

**PENJELASAN MENGENAI KESAN BAHAN PERENCAT DARI HASILAN
SEMULAJADI MALAYSIA KE ATAS TITISAN SEL TUMOR KOMPLEKS
SKLEROSIS TUBEROUS**

ABSTRAK

Perencat *mammalian target of rapamycin* (mTOR) adalah rawatan utama untuk angiomiolipoma berkaitan kompleks sclerosis tuberosus (TSC). Everolimus telah diluluskan oleh Pentadbiran Makanan dan Dadah Amerika Syarikat (USFDA) untuk rawatan angiomiolipoma berkaitan TSC yang tidak memerlukan pembedahan segera. Walaubagaimanapun, everolimus menunjukkan keberkesanan sederhana angiomiolipoma dan mempunyai beberapa batasan lain. Kajian ini bertujuan mengenalpasti potensi perencat mTOR daripada sumber tempatan Malaysia sebagai alternatif kepada everolimus dalam merawat angiomiolipoma. Tahap pertama kajian ini melibatkan penyaringan maya dan dok menggunakan pendekatan *in silico* untuk mengenal pasti perencat mTOR yang berpotensi daripada pangkalan data tempatan NADI. AutoDock Vina digunakan untuk menyaring maya everolimus dan lebih daripada 4000 bahan (ligan) daripada lebih 360 spesies tumbuhan secara serentak terhadap FKBP5 dan FRB-domain mTOR. Everolimus bertindak sebagai kawalan positif dan penanda aras untuk pemilihan selanjut perencat mTOR yang berpotensi. AutoDock 4.2.6 kemudiannya digunakan untuk mengenal pasti kedudukan pengikatan setiap bahan dengan skor dok terendah. Tahap kedua kajian melibatkan bioasai berasaskan sel yang menggunakan titisan sel UMB1949 sebagai model TSC untuk mengesahkan penemuan *in silico* dan menilai toksisiti bahan secara *in vitro*. Tahap terakhir kajian melibatkan penilaian kesan bahan pada ekspresi gen di jalur mTOR menggunakan teknik RT-qPCR. Kajian menemui dua bahan bioaktif daripada *Centella*

asiatica, asiatikosid dan asid asiatik, mempunyai skor dok yang lebih rendah dan lebih dekat kepada everolimus (-11.86 kcal/mol) dan memenuhi kriteria pemilihan sebagai perencat mTOR yang berpotensi. Nilai IC_{50} asiatikosid dan asid asetik adalah masing-masing $300\text{ }\mu\text{M}$ dan $60\text{ }\mu\text{M}$. Nilai-nilai ini lebih tinggi daripada everolimus ($29.5\text{ }\mu\text{M}$) tetapi mereka menunjukkan aktiviti antiproliferatif setanding secara *in vitro*. *CAB39*, *PRKCE*, *RRAGC*, dan *RPS6KA5* adalah dikawal atur menaik oleh kesemua bahan, everolimus, asiatikosid dan asid asetik. *DEPTOR* adalah dikawal atur menurun oleh kesemua bahan. *VEGFC* (dikawal atur menurun oleh asiatikosid) dan *IGFBP3* (dikawal atur menurun oleh everolimus dan asid asetik) juga telah dipilih sebagai gen yang difokuskan kerana peranannya yang dilaporkan membantu angiogenesis tumor dan apoptosis, dan bermungkinan merencat mTOR. Ini adalah kajian pertama yang bertujuan mengenal pasti kemungkinan potensi terapi asiatikosid dan asid asiatik dalam model penyakit TSC yang mensasarkan perencatan mTOR. Penemuan ini, dengan kombinasi penemuan *in silico* kami, seharusnya menyediakan asas untuk lebih banyak penyelidikan tentang mekanisme tindakan, keselamatan dan keberkesanan bahan ini sebagai perencat mTOR.

**ELUCIDATING THE EFFECTS OF mTOR INHIBITORS FROM
MALAYSIAN NATURAL PRODUCTS ON TUBEROUS SCLEROSIS
COMPLEX CELL LINE**

ABSTRACT

Mammalian target of rapamycin (mTOR) inhibitors are a highly recommended first-line therapy for tuberous sclerosis complex (TSC)-associated angiomyolipoma. Everolimus has been approved by the United States Food and Drug Administration (USFDA) for treatment of TSC-related angiomyolipoma that do not require urgent surgery. However, everolimus showed only modest efficacy for angiomyolipoma and has several other limitations. This present study aimed to identify potential mTOR inhibitor from Malaysian local sources as an alternative to everolimus in treating angiomyolipoma. The first stage of this present study involved virtual screening and docking using in silico approach to identify potential mTOR inhibitors from a local NADI database. AutoDock Vina was applied for virtually screening everolimus and more than 4000 substances (ligands) from over 360 plants species simultaneously against FKBP5 and FRB-domain of mTOR. Everolimus acted as positive control and benchmark for further selection of potential mTOR inhibitors. AutoDock 4.2.6 was later applied to identify the binding pose of each substance with the lowest docking score. The second stage of the study involved cell-based bioassays using UMB1949 cell line as TSC model to validate the in silico finding and evaluate the toxicity of the substances in vitro. The last stage of the study involved evaluation of the effects of substances on genes expression in the mTOR pathway using reverse transcription quantitative real-time polymerase chain reaction (RT-qPCR) technique. It was

discovered asiaticoside and asiatic acid, two bioactive substances from *Centella asiatica* have lower and closer docking score to everolimus (– 11.86 kcal/mol) and have met the selection criteria as potential mTOR inhibitors. IC₅₀ values of asiaticoside and asiatic acid were 300 µM and 60 µM, respectively. These values were higher than everolimus (29.5 µM) but they exhibited comparable antiproliferative activities in vitro. *CAB39*, *PRKCE*, *RRAGC*, and *RPS6KA5* were upregulated by all three substances, everolimus, asiaticoside and asiatic acid. *DEPTOR* was commonly downregulated by all three substances. *VEGFC* (downregulated by asiaticoside) and *IGFBP3* (downregulated by everolimus and asiatic acid) were also selected as genes of interest due to their reported roles in aiding tumour angiogenesis and apoptosis, and possible mTOR inhibition. This is the first study to look at identifying possible therapeutic potentials of asiaticoside and asiatic acid in TSC disease model that targets mTOR inhibition. These findings, in combination with our in silico findings, provide a basis for more research into the mechanisms of action, safety, and efficacy of these substances as mTOR inhibitors.

CHAPTER 1

INTRODUCTION

1.1 Research background

Tuberous sclerosis complex (TSC) is a rare, multi-system genetic disorder that causes non-cancerous (benign) tumours to develop in the brain and on other vital organs including the kidneys, heart, eyes, lungs, and skin. It has been well established that mutations in either *TSC1* or *TSC2* are the cause of the TSC in 85% of the patients. Although curative therapy is still largely elusive, mTOR inhibition has been a hallmark therapeutic target for tumour manifestations of TSC. Rapamycin, a United States Food and Drug Administration (USFDA)-approved immunosuppressant drug has been showed to substitute the role of hamartin/tuberin protein complex (encoded respectively by *TSC1* and *TSC2*) in inhibiting mTOR activity towards control of cell growth and proliferation. In addition, the efficacy of rapamycin in shrinking tumours related to TSC manifestations has been demonstrated. Rapamycin, naturally produced by the soil bacteria of *Streptomyces hygroscopicus* isolated from the Easter Island, is currently hardly accessible to TSC Malaysian patients as well as other patients in worldwide for its USFDA-approved usage. This is because of, until now, rapamycin has not been approved by USFDA for treating any TSC manifestation despite extensively used for treating facial angiofibromas (Canpolat et al., 2014) and subependymal giant cell astrocytoma (SEGA) (Sparagana et al., 2010). The reasons are due to a significant progression in facial angiofibromas after rapamycin therapy discontinued (Canpolat et al., 2018) and rapamycin has no effect on optic nerve tumour for subependymal giant cell astrocytoma (SEGA) (Sparagana et al., 2010).

Besides, it was found out that rapamycin has poor pharmacokinetics and this led to the development of everolimus. Due to its superior efficacy, everolimus has been approved by USFDA for several cancer types such as advanced breast cancer, advanced renal cell carcinoma (RCC), pancreatic neuroendocrine tumours (PNETs) and selected manifestations of TSC such as renal angiomyolipoma (patients not preferring urgent surgery) and SEGA (patients need therapeutic intervention but cannot be curatively resected) (Lebwohl et al., 2013). Meanwhile, in Malaysia, everolimus has been used in combination with lenvima for treating adult patients with advanced renal cell carcinoma (RCC) following before vascular endothelial growth factor (VEGF)-targeted therapy (National Pharmaceutical Regulatory Agency (NPRA), 2018).

Malaysia has been a place where tremendously numerous natural substances can be derived, be it from plants, bacteria or animals. Following this, the Universiti Sains Malaysia (USM) School of Pharmaceutical Sciences has developed a resourceful database where information of thousands of natural substances stored could be traced for their homology to other pharmaceutical substances in use and their activity towards a certain therapeutic target. This database is known as NADI (Natural Product Discovery) and the present study used this database to discover the promising mTOR inhibitors as an alternative for standard treatment, everolimus, for treating TSC.

Therefore, the present study aimed to identify the potential mTOR inhibitors using the *in silico* analyses. Only a few top substances with the lowest docking score than everolimus that resulted from the *in silico* analyses were subjected to the cell-based bioassays for cytotoxicity test. Furthermore, the significant effects of these selected substances on the gene expression levels in the mTOR pathway were determined and

validated using reverse transcription quantitative real-time polymerase chain reaction (RT-qPCR). The gene functions were determined using bioinformatics analysis.

1.2 Rationale of the study

Everolimus had already been licensed by the USFDA and European Medicines Agency (EMA) as the standard drug for the treatment of inoperable TSC-related brain and kidney tumours. However, patients do not have good access to this treatment because of its high cost i.e., £28,000 per year per patient (2016). In Malaysia, the current price of everolimus (10 mg per tablet) is between RM 144.58-RM1,126.49 for each tablet (depends on the manufacturer). Besides, everolimus treatment has numbers of limitations. First and foremost, the use of everolimus as monotherapy for treating cancer resulted in modest efficacy as it exerted cytostatic rather than cytotoxic effect (Meric-Bernstam and Gonzalez-Angulo, 2009). Everolimus also failed to completely block mTORC1-mediated signalling events. Like other mTOR inhibitors, resistance towards everolimus due to the existence of feedback loops (Carew et al., 2011) has also been reported. Everolimus has been associated with several side effects such as pneumonia, nasopharyngitis, sinusitis, amenorrhoea, stomatitis, upper respiratory tract infections, disturbed wound healing, acne and laboratory abnormalities such as hypercholesterolemia, hypertriglyceridemia and neutropenia (Trelinska et al., 2015; Sadowski et al., 2016). Therefore, the present study aimed to determine the potential mTOR inhibitor to solve the limitations of the current standard treatment for TSC patients. The present study hypothesised that potential Malaysian-derived mTOR inhibitors could be screened and acquired from the NADI database utilising a virtual

screening method and differential gene expression in the mTOR pathway could be determined.

1.3 Objectives of the study

1.3.1 General objective

The general objective of this present study was to elucidate the effects of Malaysian-Derived mTOR inhibitor on Tuberous Sclerosis Complex (TSC) cell line.

1.3.2 Specific objectives

- 1) To identify Malaysian-Derived mTOR inhibitor substances; substances with lower docking score than everolimus and/or substances targeting inhibition of mTOR activity.
- 2) To determine the IC_{50} of everolimus and selected Malaysian-Derived mTOR inhibitor substances on human Tuberous Sclerosis cell line (UMB1949).
- 3) To determine the expression of selected genes along the mTOR pathway following treatment with everolimus and selected Malaysian-Derived mTOR inhibitor substances on human Tuberous Sclerosis cell line (UMB1949).
- 4) To validate the expression of selected genes found to be highly modulated along the mTOR pathway.

CHAPTER 2

LITERATURE REVIEW

2.1 Tuberous Sclerosis Complex (TSC)

TSC (OMIM 191100) (Rosset et al., 2017) is a rare autosomal dominant inherited (Lin et al., 2019) multisystemic disorders characterized by the growths of hamartomas, generally affecting multiple organs such as the brain, skin, kidney, heart and lungs (Huang and Manning, 2008; NINDS 2013). TSC is also known as *epiloia* or Bourneville-Pringle disease (Rodrigues et al., 2012). Pathophysiologically, TSC is caused by the mutation of either one of two tumour suppressor genes, *TSC1* (tuberous sclerosis complex 1) or *TSC2* (tuberous sclerosis complex 2), which functionally encode hamartin and tuberin, respectively (European Chromosome 16 Tuberous Sclerosis Consortium, 1993; van Slegtenhorst et al., 1997; Curatolo et al., 2008; Franz et al., 2010; Bolton et al., 2015; DiMario et al., 2015) and this event will trigger activation of the mechanistic or mammalian target of rapamycin (mTOR) signalling pathway, leading to uncontrolled cell growth/proliferation and finally cause the development of hamartomas in multiple organs, influencing the role of these organs (Huang and Manning, 2008; Mackeigan and Krueger, 2015; Gruber et al., 2019; Lin et al., 2019; Štefániková et al., 2019). Despite TSC being categorized as a rare disorder, it was estimated 1.5 million individuals were affected by TSC globally (Kingswood and de Vries, 2015). TSC affected both genders equally (Kingswood and de Vries, 2015; Rosset et al., 2017), all racial and ethnic groups (Tsai and Crino, 2012; Kingswood and de Vries, 2015; Rosset et al. 2017).

It was reported that the incidence of live births approximately 1:6000 to 1:10,000 (Osborne et al., 1991; Crino et al., 2006; Devlin et al., 2006; Curatolo et al., 2008; Orlova and Crino, 2010), while the general estimation of TSC prevalence was between 1: 14,000 and 1: 25,000 (Devlin et al., 2006; Hong et al., 2009). Specifically, based on the evidence, the TSC prevalence decreases as age increases such as for those aged less than 6 years, at 12 years and at 18 years old, their prevalence was 1: 14,000, 1: 19,000 and 1: 24,000, respectively (Devlin et al., 2006; Hong et al., 2009).

It was reported that one-third of the cases are familial cases, in which the disorder follows an explicit dominant inheritance pattern, while two-thirds of the cases are sporadic due to the *de novo* germline mutations in one of the *TSC* (Osborne et al., 1991; Dabora et al., 2001). The latter was manifested by a high rate of spontaneous mutations (Dabora et al., 2001; Gao et al., 2018). In familial cases, both genes contributed to the same frequency of mutations (Povey et al. 1994; Jones et al. 1997) whereas in *de novo* cases, *TSC2* mutations are 2 to 10 times more common than *TSC1* mutations (Jones et al., 1999; Nijda et al., 1999; Dabora et al., 2001; Langkau et al., 2002; Rosset et al., 2017). This might be due to the GAP domain (exon 35 – 39) of *TSC2* a target for missense mutations (Maheshwar et al., 1997). The frequency of *de novo TSC1* mutations is lower than *TSC2* mutations due to a few factors such as less complexity, smaller size structure of genomic locus, rarity of missense, large DNA rearrangements and splice site mutations (Kwiatkowski, 2003). In addition, *TSC1* mutations are also linked to less severe TSC phenotype compared to *TSC2* mutations (Jones et al., 1999; Dabora et al., 2001).

According to Rosset et al (2017), approximately 80-95% of types of mutations present in *TSC1* and *TSC2* mutations are small mutations such as missense, small deletions, nonsense, splicing site mutations and small insertions. Only 5-20% represents large deletions, large duplications or complex rearrangements (Rosset et al., 2017) which were reported exclusively in *TSC2* (Sandra et al., 2001). *TSC1* had three hotspot regions, which were identified as exons 8, 15, and 18. Meanwhile, the most frequently mutated areas of *TSC2* were exons 29, 33, and 40 (Jiangyi et al., 2020).

2.2 TSC genes, their protein products and TSC protein complex

TSC1 (van Slegtenhorst, 1997) and *TSC2* (ECTSC, 1993) were identified as causal genes for TSC disorder by the positional cloning approach. The cytogenetic location of *TSC1* and *TSC2* were 9q34.13 and 16p13.3, respectively (Salussolia et al., 2019). *TSC1* comprises a 23 exons gene, where exons 1 and 2 make up the 5' untranslated region (do not affect the encoded protein) (Ali and Kumar, 2003) and exons 3 – 23 encode an 8.5 kb mRNA and hamartin (Avgeris et al., 2017). Hamartin comprises 1,164 amino acids and its molecular mass is 130 kDa (Salussolia et al., 2019). Surprisingly, there is no other vertebrate protein that homology to hamartin (Rosset et al., 2017). Hamartin consists of a putative transmembrane domain at amino acids 127–144 (Jozwiak, 2006) implying that it is membrane-bound and has a large coiled-coil domain amino acid 730 – 996 (Jozwiak, 2006; Napolioni and Curatolo, 2008). This domain is required for protein-protein interactions between hamartin and tuberin (Van Slegtenhorst et al., 1998) and also the binding of TBC1D7 to hamartin for stabilization of hamartin dimerization (Gai et al., 2016; Qin et al., 2016). Hamartin has been suggested to regulate cell adhesion due to its interaction with the ezrin-radixin-moesin

(ERM) family member proteins and activates the small-GTP binding protein Rho (Lamb et al., 2000) (Figure 2.1). It was described as hamartin to be localized to the centrosome (Napolioni and Curatolo, 2008). A major function of hamartin is to stabilize the hamartin tuberlin complex and facilitate the GTPase-activating function of tuberlin in the complex (Han and Sahin, 2011).

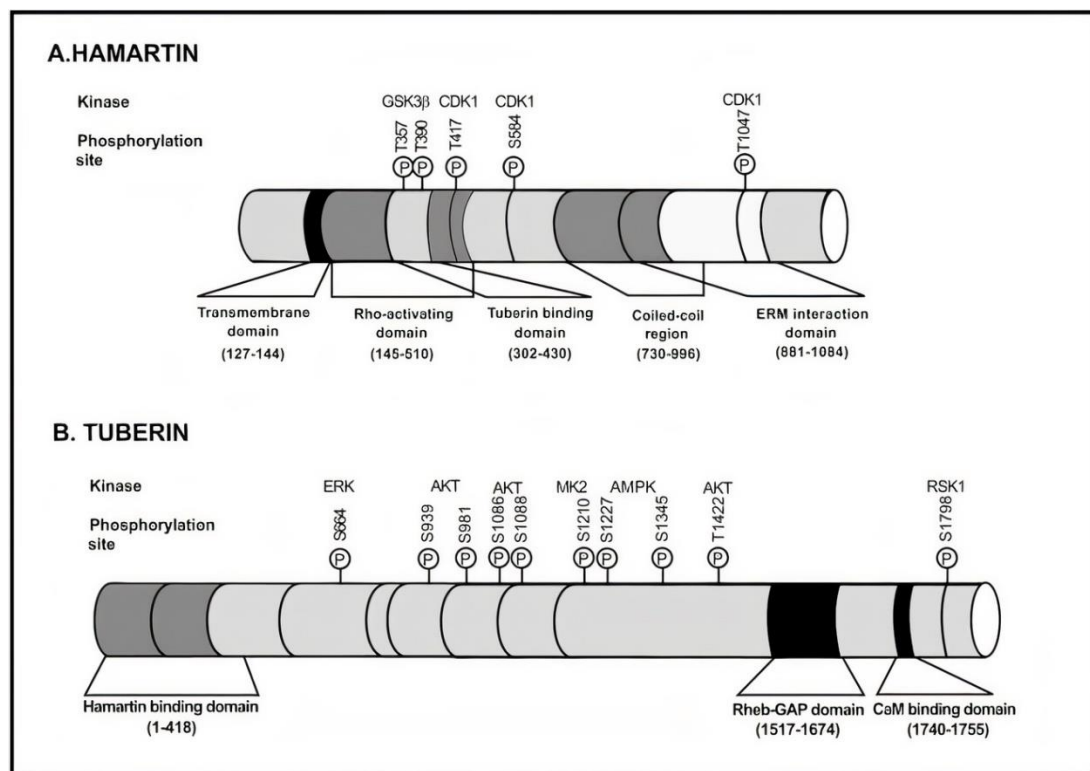


Figure 2.1: The detailed structures of hamartin and tuberlin (Adapted from Napolioni and Curatolo, 2008)

TSC2 comprises 42 exons gene, where exon 1 does not has a coding sequence and located in the 5'untranslated region (Ekong et al., 2016), exons 2–42 encoding the functional protein (Ekong et al., 2016) and exons 25, 26 and 31 are subject to alternative splicing (Cheadle et al., 2000). *TSC2* functions encoding a 5.5 kb mRNA and tuberlin. Tuberlin comprises 1807 amino acids and its molecular mass 198 kDa. A

region spanning amino acids 1517-1674 and encoded by exons 34 – 38 show significant homology to the Ras superfamily GTPase-activating proteins (GAPs) human rap1 GAP and murine Spa1 (Figure 2.1) (ECTSC, 1993; Maheshwar et al., 1997). Since tuberin is a GTPase activating protein, it regulates the GTP binding and hydrolysing activity of the Ras superfamily of proteins (Rosset et al., 2017) and plays a vital role in the regulation of cell cycle progression, differentiation and development (Sudarshan et al., 2019). Interestingly, based on mutational analysis of *TSC2* from TSC patients, it was advocated that the GAP domain region of tuberin is critical for its function (Niida et al., 1999). In addition, tuberin has a hamartin binding domain (amino acids 1 – 418) (Benvenuto et al., 2000) and it is important to retain hamartin localized in the cytosol in the form of soluble (Nellist et al., 1999). Tuberin has been reported to be localised to the cytosol and the membrane fraction within the cytoplasm and the nucleus (Napolioni and Curatolo, 2008). Hamartin and tuberin are co-expressed in cells of few organs such as the brain, kidney, pancreas and lung (Napolioni and Curatolo, 2008). Most hamartin and tuberin are localized in the cytosol (Nellist et al., 1999) and a small fraction of them could be found in the Golgi, early endosomes and associated with membrane fraction or cytoskeleton (Plank et al., 1998; Nellist et al., 1999).

TSC1 and TSC2 are associated with the third protein, Tre2-Bub2-Cdc16 (TBC) 1 domain family, member 7 (TBC1D7) and formed a heterotrimeric complex namely, TSC protein complex (Figure 2.2). TSC1 is needed as a stabilizer for TSC2 (Huang and Manning et al., 2008) and TBC1D7 (Napolioni and Curatolo, 2008) and also to avoid *TSC2* ubiquitin-mediated proteasomal degradation (Chong-Kopera et al., 2006; Hu et al., 2008) or TSC2 sequestration by 14-3-3 binding (Li et al., 2002;

Shumway et al., 2003). The function of TSC2 will be inhibited if 14-3-3 is associated with TSC2 (Li et al., 2002). Based on the biochemical characterization report, it was suggested TBC1D7 as a third protein component of the TSC protein complex (Salussolia et al., 2019). In the TSC complex, TBC1D7 stabilizes the hamartin dimerization through the binding to the coiled-coiled fragment of hamartin (Gai et al., 2016; Qin et al., 2016). The interaction between TSC1-TSC2-TBC1D7 contributes to the stabilization of them as “Rhebulator” complex (Sato et al., 2010; Dibble et al., 2012). Besides, TBC1D7 vital for the interaction between TSC1 and TSC2 and needed for the appropriate regulation of Rheb and mTORC1 by cellular growth condition as well (Dibble et al., 2012). It was reported that the knockdown of TBC1D7 caused the reduction of association TSC1 and TSC2. This reduction leads to decreased Rheb-GAP activity and elevated mTORC1 activity, hence, increased cell growth and detained induction of autophagy under low energy conditions (Dibble et al., 2012). Apart from this, mTORC1 signalling also elevated by overexpression of TBC1D7 (Nakashima et al., 2007). mTOR activation is inhibited by the TSC protein complex through the action of the GTPase-activating protein (GAP) domain in TSC2 (Salussolia et al., 2019). TSC1 binds to TSC2 through the C-terminal coiled-coil domain and the N-terminal TSC2-interacting core domain (Nellist et al., 1999; Sun et al., 2013; Lima et al., 2014; Gai et al., 2016). TSC complex is a critical negative regulator of the mechanistic target of rapamycin (mTOR), a master regulator to many cellular functions such as cell growth and proliferation (Gao et al., 2002; Inoki et al., 2002; Tee et al., 2002) (Figure 2.2).

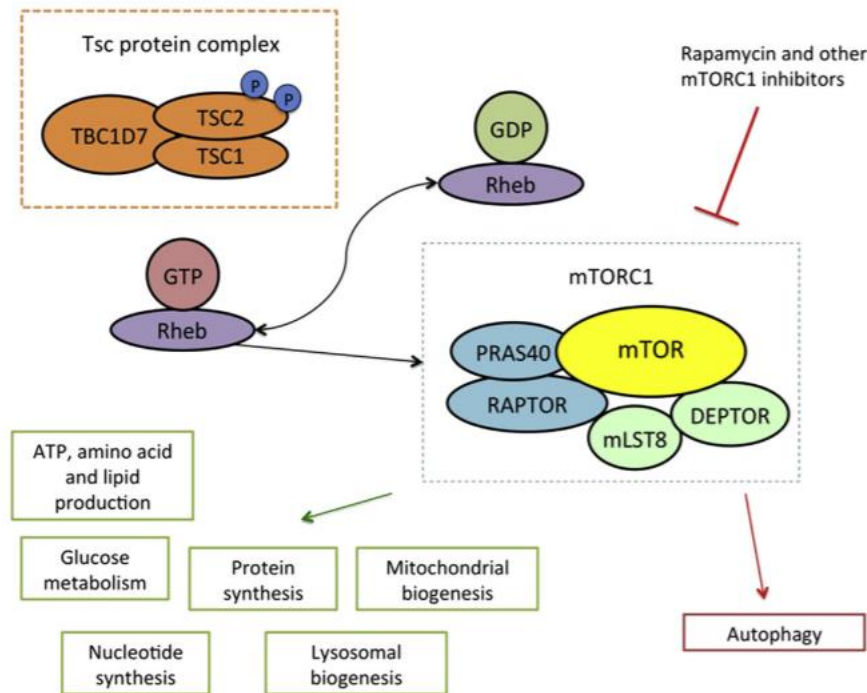


Figure 2.2: The subunits of TSC protein complex, mTORC1 subunits and its downstream functions (Adapted from DiMario et al., 2015)

2.3 mTOR complexes and their function

mTOR protein is a 289-kDa serine-threonine kinase that belongs to the phosphoinositide 3kinase (PI3K)-related kinase family and is conserved throughout evolution (Laplane and Sabitini, 2009). Figure 2.3 shows the detailed domain of mTOR. Localization of mTOR is found in the cellular cytoplasm as a complex with other molecules (Strimpakos et al., 2009). mTOR plays an integral role in the coordination of metabolism, protein synthesis, cell growth, and proliferation (Feng et al., 2020). It acts as a molecular sensor to maintain metabolism and cellular homeostasis and integrate environmental signals by altering the cellular and metabolic processes (Soliman, 2005; Foster and Finger, 2010). The reported studies have implicated mTOR as a cell cycle progression and a central regulator of metabolism,

cellular proliferation, and growth (Laplane and Sabatini, 2009; Duvel et al., 2010; Saxton and Sabatini, 2017; Feng et al., 2020). mTOR regulates cell growth by controlling autophagy, mRNA translation, metabolism and ribosome biogenesis (Guertin and Sabatini, 2005; Sarbassov et al., 2005; Wullschleger et al., 2006). mTOR pathway is activated during various cellular processes (such as tumour formation and angiogenesis, insulin resistance, adipogenesis and T-lymphocyte activation) and is deregulated in chronic diseases including diabetes, insulin resistance, obesity and cardiovascular disease (McMahon et al., 2011) and various types of cancer (Arva et al., 2012).

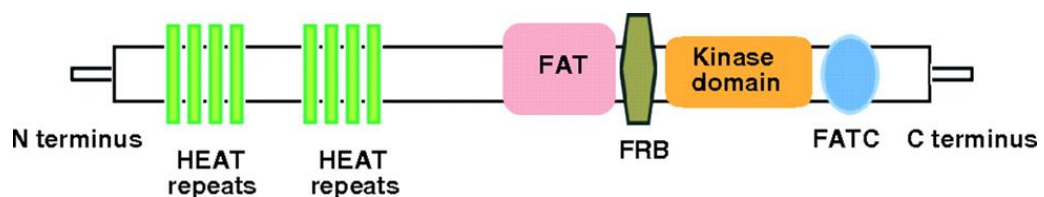


Figure 2.3: Schematic representation of mTOR domain. mTOR is an evolutionarily conserved serine-threonine that belongs to the phosphatidylinositol-3-kinase-related kinase (PIKK) family. Structurally, the N-terminal half of mTOR protein possesses two identical HEAT (Huntington, Elongation factor 3A, a subunit of PP2A, and TOR1) repeats and functionally in mediating the formation of a multimeric complex with other protein targets. Next to HEAT repeats, is the FAT (FRAP, ATM and TRRAP) domain and contributing to the active conformation of the kinase domain. FRB (FKBP12-rapamycin-binding) domain is significant to TOR family kinase because the hydrophobic cleft of this domain promotes its interaction with the FKBP-rapamycin complex. Indirectly, the FRB domain has been proposed as a possible regulatory domain of mTOR activity. The FRB domain is followed by the catalytic kinase domain. Lastly, the FATC (FAT C-terminus) domain at the C-terminus possess the homology sequence to the FAT domain and it plays the same role as the FAT domain as well (Adapted from Russell et al., 2011)

mTOR plays its main cellular functions by forming two distinct protein complexes, mTORC1 and mTORC2, through assembly with specific adaptor proteins (Wullschleger, et al., 2006; Kapahi et al., 2010). These two protein complexes with different composition, control mTOR functions (Verhoef et al., 1999; Eussen et al., 2000). Both mTOR complexes are large; where mTORC1 and mTORC2 comprised of six and seven known protein components, respectively (Laplane and Sabatini, 2012). Figure 2.4 illustrates the components, specific inputs and function for each mTOR complex. Both mTOR complexes share four similar components: mTOR subunit, mLST8 (mammalian lethal with Sec13protein8, also known as G β L), which is a positive regulator, DEPTOR (DEP domain-containing mTOR-interacting protein), which works as the negative regulator and Tti1/Tel2 complex, the complex responsible for stabilization of mTOR and regulation of the PIKKs stability (Kaizuka et al., 2010). Specifically, mTORC1 associated with Raptor (regulatory-associated protein of mTOR), a positive regulator involved in substrate recruitment, and PRAS40 (proline-rich Akt substrate of 40kDa), the component responsible for mTORC1 inhibition, (Sancak et al., 2005). While, mTORC2 is associated with mSIN-1 (mammalian stress-activated protein kinase interacting protein), which is necessary for the assembly of the complex, Rictor (rapamycin-insensitive companion of mTOR), an essential player in the activation of the interaction between mTORC2 and tuberous sclerosis complex 2 (TSC2), and PROTOR-1 (protein observed with RICTOR-1), which has been showed to bind to RICTOR (Eussen, 2000; Verhoef, 1999). Recently it was discovered rapamycin-resistant mTOR complex, mTORC3, as one of members of mTOR complex (Harwood et al., 2018). However, little information regarding mTORC3 is revealed for this time being. It was reported, mTOR interacts with ETS variant transcription factor 7 (ETV7) to form a complex and promote cell proliferation

(Harwood et al., 2018). ETV7 is a member of the PNT (pointed) domain-containing ETS (E26 transformation-specific) family of transcription factors (Potter et al., 2000) and it is present in all vertebrates except a subset of rodents such as mouse (Harwood et al., 2018). Overexpression of ETV7 was reported associated with tumourigenic transformation in mice (Cardone et al., 2005; Carella et al., 2006). Despite Raptor or Rictor absent as one of mTORC3 component, it is still being able to phosphorylate target proteins such as S6K1, 4E-BP1 and Akt. Surprisingly, even-though overexpression of ETV7 was observed in U937 cells, it failed to elevate mTORC3 formation. This scenario is different compared to scenario of mTORC1 and mTORC2. In mTORC1 and mTORC2, overexpression of Raptor and Rictor respectively, directly elevates the formation and activity of both mTOR complexes (Sarbasov et al., 2004; Masri et al., 2007; Bashir et al., 2012). Therefore, it is postulated that, the formation and activity of mTORC3 might be controlled via post-translational modifications (PTMs) (Harwood et al., 2018). PTMs are covalent processing processes that alter a protein's characteristics through proteolytic cleavage and the addition of a modifying group, including methyl, phosphoryl, glycosyl, and acetyl (Ramazi et al., 2020). PTMs exert a major influence on the structure and dynamics of proteins in a wide variety of biological processes, including gene expression regulation, signal transduction, cell cycle control, DNA repair, and gene activation (Strumillo and Beltrao, 2015; Wang et al., 2015; Xu and Chou, 2016; Wei et al., 2017). mTOR signalling has been showed to be controlled by PTMs such as phosphorylation, ubiquitination, glycosylation, and acetylation (Azim et al., 2010; Zoncu et al., 2011; Yin et al., 2021).

mTORC1 is regulated by various signals, such as nutrients, growth factors, oxygen, energy status, and cellular stress (Liao et al., 2011). mTORC1 master regulation of

protein synthesis, proliferation, cell survival, autophagy, ribosome biogenesis, angiogenesis, mitochondrial biogenesis, migration, metabolism, invasion, and metastasis by phosphorylation of ribosomal protein S6 kinase 1 (S6K1) and eukaryotic initiation factor 4E (eIF4E)-binding protein 1 (4EBP1) (Sarbasov et al., 2005; Zhang et al., 2005). Until recently, it has been assumed that mTORC2 is largely resistant to regulation by nutrients and is activated by growth factors only (Soliman, 2015).

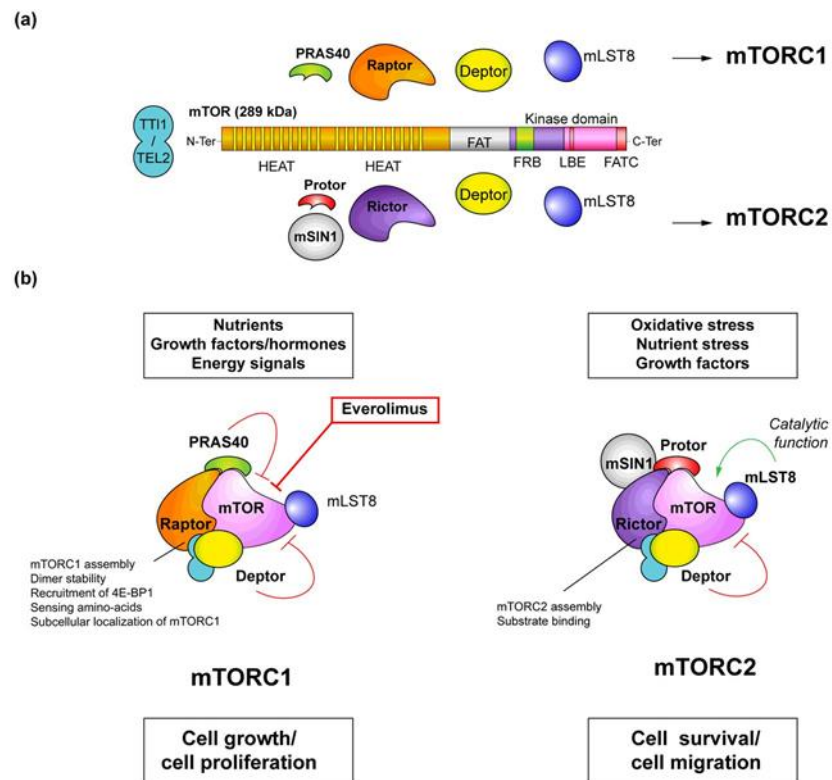


Figure 2.4: mTOR complexes: mTORC1 and mTORC2 mTOR forms two distinct structurally and functionally complexes: mTORC1 and mTORC2. (a) The specific catalytic subunit that form mTORC1 and mTORC2. (b) mTORC1 and mTORC2 stimulate by different inputs and responsible for different downstream applications (Adapted from Saran et al., 2015)

mTORC2 functions in cell proliferation, survival, polarity, cell-cycle progression, actin remodeling, and cell survival through the regulation of protein kinase C α (PKC α) and serum and glucocorticoid-induced protein kinase 1 (SGK1) (Polak and Hall, 2006; García-Martínez and Alessi, 2008). Few studies showed that mTORC2 was associated with ribosomes and thus may be involved in protein synthesis (Zinzalla et al., 2011). The PI3K pathway was showed to activate mTORC2, and it seems to activate the TSC1/2 complex as well. mTORC1 seems to inhibit mTORC2 via phosphorylation of Rictor, suggesting that mTORC1 and mTORC2 are functionally interconnected (Zinzalla et al., 2011).

2.4 Clinical features and classification of TSC

Diagnosis of TSC is according to the revised and updated clinical diagnostic criteria for TSC, established in 2012 (Wataya-Kaneda et al., 2017; Ebrahimi-Fakhari et al., 2018). Based on Table 2.1, the diagnostic criteria for TSC are divided into two which are genetic and clinical diagnostic criteria. The inclusion of genetic testing in revised TSC diagnostic criteria is significant as identification of pathogenic mutation in *TSC1* or *TSC2* in normal tissue is adequate for diagnosis and clinical manifestations not necessary. For clinical diagnostic criteria, TSC is diagnosed based on the presence of major and minor features of the disorder. A definite diagnosis is made on clinical grounds, two major features or one major plus two or more minor features are required to make a diagnosis. Meanwhile, possible TSC can be scrutinized when one major feature or two or more minor features are present (Palavra et al., 2017). TSC-related phenotypes are highly variable such as in some individuals, they suffered from infantile spasms and severe developmental delays at early life, while the others may remain undiagnosed until their family member is identified (Farach et al., 2019). In

addition, the clinical manifestations of TSC may vary greatly among family members (Jozwiak et al., 2000; Curatolo et al., 2008; Curatolo and Maria, 2013; Salussolia et al., 2019).

Table 2.1: Revised and updated clinical diagnostic criteria of TSC (Northrup et al., 2013)

A. Genetic diagnostic criteria	
The identification of either a <i>TSC1</i> or <i>TSC2</i> pathogenic mutation in DNA from normal tissue is sufficient to make a definite diagnosis of TSC. A pathogenic mutation is defined as a mutation that clearly inactivates the function of the TSC1 or TSC2 proteins.	
B. Clinical diagnostic criteria	
Major features	Minor features
Facial angiofibromas (≥ 3) or fibrous cephalic plaque	Dental enamel pits (> 3)
Ungual fibromas (≥ 2)	Intraoral fibromas (≥ 2)
Hypomelanotic macules (≥ 3 , at least 5 mm diameter)	Retinal achromic patch
Shagreen patch	Nonrenal hamartomas
Multiple retinal hamartomas	“Confetti” skin lesions
Cortical dysplasias*	Multiple renal cysts
Subependymal nodule (SEN)	
Subependymal giant cell astrocytoma (SEGA)	
Cardiac rhabdomyoma	
Lymphangiomyomatosis (LAM) ⁺	
Angiomyolipomas (≥ 2) ⁺	

*Includes tubers and cerebral white matter radial migration lines.

⁺ A combination of the two major clinical features (lymphangiomyomatosis and angiomyolipomas) without other features does not meet the criteria for a definite diagnosis.

2.5 The mTOR signalling pathway of TSC

Currently, a plethora of upstream inputs is known to regulate mTORC1 activity including growth factors (Figure 2.5). The activation of growth factors such as insulin and IGF-1 induce binding and phosphorylation of insulin receptor substrate 1 (IRS-1). These binding stimulate the PI3K pathway, where, phosphorylation of phosphatidylinositol-(4,5)-biphosphate (PtdIns (4,5)P₂ (PIP₂) by activated PI3K leads to PtdIns(3,4,5)P₃ (PIP₃) at the plasma membrane. PIP₃ then activated PDK1 (Alessi et al., 1997; Stokoe et al., 1997) and also recruits Akt (PKB) to the plasma membrane (Pearce et al., 2010). The phosphorylation of Akt at T308 residue by PDK1 leads to partial activation and additional phosphorylation at hydrophobic motif site S473 by PDK2 is required to complete the activation of Akt (Toker and Newton, 2000).

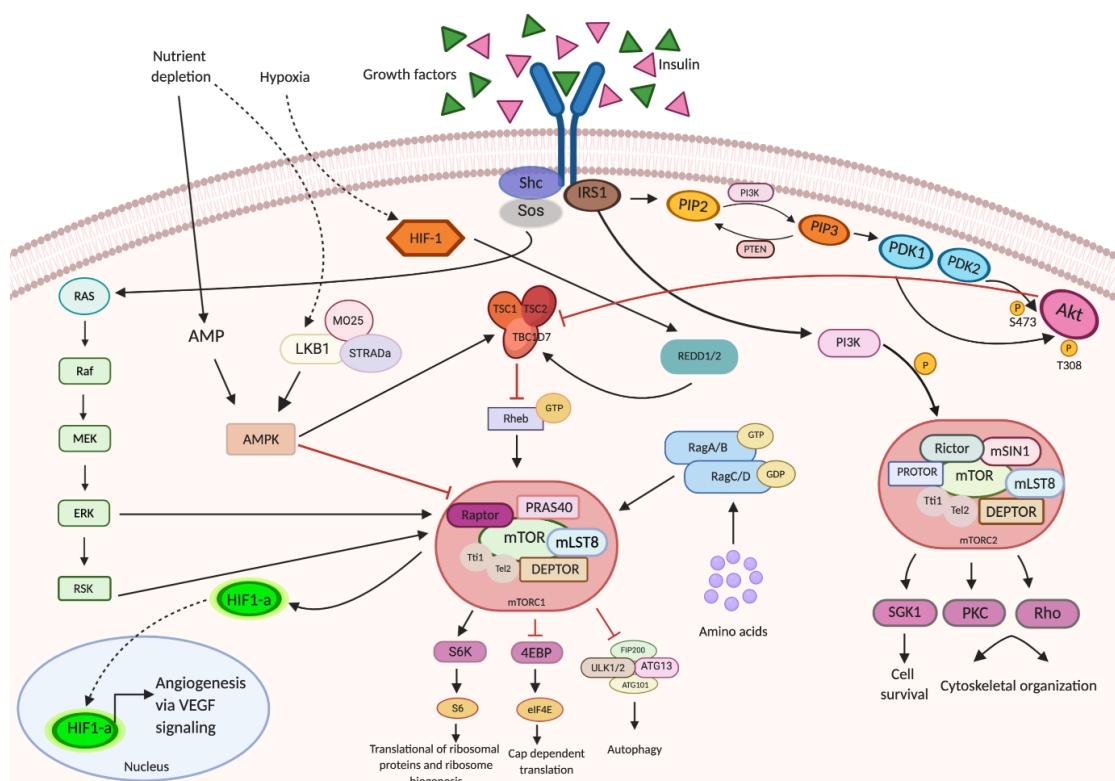


Figure 2.5: The inputs and downstream functions in the mTOR pathway that responsible for TSC (Adapted from BioRender.com)

Following full activation of Akt by PDK1 and PDK2, Akt phosphorylates and inactivates the TSC1/2 complex (Potter et al., 2002). The GTPase-activating protein (GAP) domain is located in the C-terminal region of TSC2 and promotes the GTPase activity of the small GTPase Rheb (Castro et al., 2003; Garami et al., 2003; Inoki et al., 2003; Tee et al., 2003; Zhang et al., 2003). The inhibition of TSC2 increases GTP-bound Rheb and hence elevates the mTORC1 activity. Consequently, mTORC1 phosphorylates its downstream substrates such as ribosomal protein S6 kinase 1 (S6K1), 4E-BP1 and growth factor receptor-bound protein 10 (Grb10). Phosphorylation of S6K1 at T389 by mTORC1 promotes translation of ribosomal proteins and ribosome biogenesis (Bjornsti and Houghton, 2004; Fingar and Blenis, 2004; Inoki et al., 2005; Gentilella et al., 2015). Inactivation of 4E-BP1 due to phosphorylation of mTORC1 reduces the binding affinity of 4E-BP1 for eIF4E and leads to elevation translation of cap-dependent mRNAs (Bjornsti and Houghton, 2004; Fingar and Blenis, 2004; Inoki et al., 2005). ULK1 is a master regulator of autophagy induction and it is directly phosphorylated by mTORC1 (Chang and Neufeld, 2009; Jung et al., 2009; Kamada et al., 2010). ULK1/2 formed a stable complex with Atg101 (Hosokawa et al., 2009), Atg13, FIP200 (Jung et al., 2009; Behrends et al., 2010). In response to nutrient deprivation, the mTORC1-dependent phosphorylation site in ULK1/2 swiftly dephosphorylated by yet unknown phosphatases and this trigger autophosphorylation of ULK1/2 and phosphorylation of FIP200 and Atg13, and consequently initiate the autophagy (Chang and Neufeld, 2009; Hosokawa et al., 2009; Jung et al., 2009; Tchevkina and Komelkov, 2012). In the condition of starved amino acids, RagA/B and RagC/D in GDP-bound state and GTP-bound state, respectively. This phenomenon resulted in the cytoplasmic localization of mTORC1. Meanwhile, in the condition of rich with amino acids, RagA/B and RagC/D in GTP-bound and

GDP-bound states, respectively and this will lead mTORC1 translocated to lysosomes via the GTP-dependent interaction of RagA/B with Raptor. mTORC1 is activated due to the colocalization with Rheb, where also located at lysosomes. Not only Rag heterodimers are triggered by amino acids, but other proteins such as VPS34 and MAP4K3 are stimulated by amino acids and essential for the activity of mTORC1 (Byfield et al., 2005; Nobukuni et al., 2005; Findlay et al., 2007; Yan et al., 2010). ERK (also known as MAPK) signalling also can be activated by growth factors and subsequently inactivate the TSC complex and directly phosphorylate the Raptor, hence, promoting the activation of mTORC1. When the cells are in a state of poor nutrients or oxygen, negative regulation of mTORC1 activity will take place. Hypoxia condition stabilizes HIF-1 α , subsequently, REDD1/2 proteins are activated and lead to stimulation of TSC complex. Stimulation of TSC complex by nutrient depletion via the activation of AMPK will occur via an increase in AMP levels or LKB1 (also known as STK11) activation. In contrast, phosphorylation of Raptor by AMPK can directly cause the inhibition of mTORC1 activity (Groenewoud and Zwartkruis, 2013). Normally, STRAD α binds and exports LKB1 out of the nucleus and then bind to MO25 (also known as MO25 α , CAB39) to form a heterotrimeric complex that possesses an inhibitory effect on mTOR signalling via cascade phosphorylation of AMPK and TSC complex (Osborne, 2010). According to Boudeau et al (2003), MO25 was determined as a novel component of the LKB1-STRAD α complex. It contributes to the stabilization of the complex in the cytoplasm and intensifies the catalytic activity of LKB1. Not only that, MO25 acts as a scaffolding component for association with of LKB1-STRAD α complex (Zeqiraj et al., 2009). In addition, the TSC complex is stimulated in response to nutrient depletion, through the activation of AMPK via activation of LKB1 or elevation in AMP levels. Moreover, mTORC1 activity also can

be directly inhibited by AMPK via phosphorylation of Raptor (Groenewoud and Zwartkruis, 2013). Not only mTORC1 is activated by growth factors such as insulin-like growth factor 1 (IGF-1) and insulin, but mTORC2 as well. The mechanism by which growth factors activate mTORC2 remains unclear. Several studies postulated that mTORC2 is activated by growth factor via PI3K-dependent manner through an unknown mechanism (García Martínez and Alessi, 2008; Oh et al., 2010; Zinzalla et al., 2011; Fu and Hall, 2020). The main function of mTORC2 is to stimulate cell survival and regulate cytoskeletal organization through its specific substrates. mTORC2 stimulates cell survival through activation of SGK1 (Sciarretta et al., 2018). While, mTORC2 plays the role in the cytoskeletal organization through regulation of the Rho family of small GTPases (Etienne-Manneville and Hall, 2002; Jacinto et al., 2004) and PKC (protein kinase C) (Sarbasov et al., 2004). Lastly, through HIF-1 α and HIF-2 α , hypoxia plays a role as a master regulator of VEGF expression (Ferrara et al., 2003). Elevation expression of HIF-1 α resulted in the formation of HIF and VEGF (Slomiany and Rosenzweig, 2006). VEGF is a key regulator in angiogenesis (Krock et al., 2011; Takenaga, 2011). HIF-1 α is upregulated in various cancers and HIF modulates the hallmarks of tumour such as invasion, angiogenesis and glucose metabolism (Ratcliffe et al., 2000; Semenza, 2003; Soni and Padwad, 2017).

2.6 Therapeutic options for TSC

2.6.1 First-generation mTOR inhibitors

Currently, there are three generations of mTOR inhibitors and they are widely tested on numerous cancer types. The first-generation mTOR inhibitors comprised of

rapamycin (sirolimus) and its rapalogs such as everolimus (RAD001), temsirolimus (CCI-779), and ridaforolimus (AP23573; previously known as deforolimus that specifically inhibit mTORC1 (Figure 2.6). Table 2.2 shows the pharmacology of first-generation mTOR inhibitors. In 1975, Suren Sehgal and his colleagues isolated a natural macrolide from *Streptomyces hygroscopicus* that possess antimicrobial activity against *Candida albicans* found in a soil sample collected from the island of Rapa Nui (Vezina et al., 1975). Later on, it was discovered that this natural product also exhibited antiproliferative property against and potent immunosuppressive properties (Ni Bhaoighill and Dunlop, 2019) and it was named rapamycin after Rapa Nui, the indigenous name for the Easter Island (Gibbons et al., 2009). Rapamycin exerted its antiproliferative action against various transformed cell lines such as renal, osteoblastic, lymphoid, hepatic, connective tissue, central nervous system, melanocytic and myogenic. It also successfully showed antiproliferative of B and T cells transformed by EBV and HTLV-1, respectively (Molnar-Kimber et al., 1995). Furthermore, rapamycin also exhibited its antiproliferative activity against head and neck squamous cell carcinoma (HNSCC) cell lines both as monotherapy and in combination with carboplatin and paclitaxel (Aissat et al., 2008). In 1999, rapamycin was approved by USFDA for prevention of graft acute rejection in kidney transplantation due to its potent immunosuppressive action in inhibition of proliferation activated T cells stimulated by IL-2, (Huang and Houghton, 2001; Saunders et al., 2001; Benjamin et al., 2011; Rivera et al., 2011). In 2003, rapamycin was approved by USFDA in coronary-artery stents to prevent restenosis (Sehgal, 2003; Thompson, 2003; Abizaid, 2007; Benjamin et al., 2011; Lamming et al., 2013). In 2015, rapamycin was approved by USFDA for the treatment of LAM due to its antiproliferative effect (Koul and Mehfooz, 2019). Meanwhile, rapamycin exhibited

mode of immunosuppressive action through inhibition of proliferation activated T cells in response to IL-2 (Bierer et al., 1990; Dumont et al., 1990) and IL-12 (Bertagnolli et al., 1994) productions. Because rapamycin exerts its immunosuppressive effect without inhibiting calcineurin phosphatase activity, like tacrolimus and cyclosporine do, it is well tolerated and does not cause calcineurin-related adverse effects such as renal damage or hypertension (Groth et al., 1999). Not only inhibited proliferation of activated T cells, but rapamycin also inhibits relapsing experimental allergic encephalomyelitis (EAE), adjuvant arthritis (AA) and the humoral immunoglobulin E (IgE) immune response (Martel et al., 1977). Even-though rapamycin was clearly stated as one of the mTORC1 inhibitors, a high concentration of rapamycin (Shor et al., 2008) and depending on cell type (Willems et al., 2012), can block mTORC2 activity hence leads to mTORC2 inhibition. Not only that, some studies revealed prolonged treatment with rapamycin possibly affect both mTORC2 and Akt (Sarbasov et al., 2006; Barilli et al., 2008).

Despite rapamycin possess lots of benefits or actions, it has unfavourable pharmacokinetics which is low bioavailability due to its poor water stability and chemical stability, and these limits its application in cancer therapy (Huang and Houghton, 2003; Zhou et al., 2010). Thus, several rapalogs with better pharmacokinetic properties, lessen immunosuppressive effects (Ballou and Lin, 2008; Rizzieri et al., 2008) and more stable were developed (Zheng and Jiang, 2015). These rapalogs include temsirolimus, everolimus and ridaforolimus. They differed from rapamycin at a single position of lactone ring (C40) where the hydrogen at C40 position is replaced by a dihydroxymethyl propionic acid ester (Elit, 2002), hydroxyethyl group (Dumont, 2001) and dimethylphosphinate (Palavra et al., 2017)

(Figure 2.6), respectively. Although rapamycin and its rapalogs differ at C40, they share the central macrolide chemical structure and due to this, they exert their effects via the same mechanism of action (Figure 2.7) (Hartford and Ratain, 2007; Zhou and Huang, 2012; MacKeigan and Krueger, 2015; Palavra et al., 2017). Upon entering the cells, each first generation of mTOR inhibitor binds to the FKBP12 to form a complex then binds to the FRB domain in the C-terminus of mTOR and hence exerting growth-inhibitory and cytotoxic effects by inhibiting mTORC1 signalling to downstream effectors (Figure 2.8) (Kunz and Hall, 1993; Chen et al., 1995; Choi et al., 1996).